ELSEVIER

Journal of Molecular Catalysis A: Chemical 160 (2000) 199–208

JOURNAL OF MOLECULAR CATALYSIS A: CHEMICAL

www.elsevier.com/locate/molcata

Biomimetical catalytic activity of iron(III) porphyrins encapsulated in the zeolite X

I.L. Viana Rosa [a,*], C.M.C.P. Manso [b], O.A. Serra [b], Y. Iamamoto [b]

[a] *Depto. de Química, Universidade Federal de São Carlos, Via Washington Luiz, Km 235, CEP: 13565-905 São Carlos, SP, Brazil*
[b] *Lab. de Bioinorgânica, Depto. de Química, FFCLRP-USP, Av. Bandeirantes 3900 CEP: 14040-901 Ribeirão Preto, SP, Brazil*

Received 1 December 1999; received in revised form 10 March 2000; accepted 10 March 2000

Abstract

The approach adopted for the obtention of zeolite-encapsulated FeP led to clean syntheses of biomimetical catalyst. The catalysts were obtained through the zeolite synthesis method, where NaX zeolite was synthesised around one of the cationic FePs: iron(III) 5,10,15,20-tetrakis(4-*N*-methylpyridyl)porphyrin (FeP**1**) or iron(III) 5-mono(2,6-dichloro-phenyl)10,15,20-tris(4-*N*-methylpyridyl)porphyrin (FeP**2**). The syntheses yielded pure FeP**1**NaX and FeP**2**NaX catalysts without any by-products blocking the zeolite nanopores. FeP**1**NaX and FeP**2**NaX efficiently catalysed the epoxidation of (*Z*)-cyclooctene by iodosylbenzene (PhIO) in DCE, giving rise to *cis*-epoxycyclooctane yields of 85% and 95%, respectively. Hydroxylation of adamantane shows a preferable alkane oxidation at the tertiary C–H bond, indicating a hydrogen abstraction through the $Fe^{IV}(O)P^{\cdot+}$ species in the initial step. The total adamantanol yields were 52% and 45% for FeP**1**NaX and FeP**2**NaX, respectively. Concerning selectivity, FeP**1**NaX and FeP**2**NaX gave an 1-adamantanol (Ad-1-ol)/2-adamantanol (Ad-2-ol) ratio of 20:1 and 11:1, respectively (after statistical correction). Therefore, these results indicate a free radical activation of the C–H bonds of adamantane as expected for *P*-450 models. In the cyclohexane oxidation catalysed by FeP**1**NaX in DCE, a cyclohexanol (C_6-ol) yield of 50% and an alcohol/ketone ratio of 10 was obtained. The hydroxylation occurs according to the so-called oxygen rebound mechanism, as expected for a *P*-450 model system. FeP**2**NaX is less selective (C_6-ol yield = 25% and alcohol/ketone = 1.2). One possible explanation is that a Russell-type mechanism involving O_2 imprisoned within the zeolite cages may be operating parallelly, generating both C_6-ol and cyclohexanone.

Keywords: Zeolites; Ironporphyrin; Ironporphyrin encapsulation; Biomimetic catalyst; Hydrocarbon oxidation

1. Introduction

Cationic metalloporphyrins (MePs) have been studied as catalysts for the oxidation of a wide range of substrates [1–6]. However, their use in homogeneous systems have the following drawbacks: (i) the porphyrin ring is liable to oxidative self-destruction; (ii) the MeP is subject to aggregation through π–π interaction; (iii) oxidation of hydrophobic organic substrates by these water-soluble complexes is difficult since the active catalytic species remains dissolved in the aqueous phase.

One way to obtain efficient, selective and easy-to-recover cationic MePs for organic substrate oxidation is the combination of electron-

* Corresponding author. Tel.: +55-16-2608208; fax: +55-16-2608350.
E-mail address: ilvrosa@dq.ufscar.br (I.L.V. Rosa).

1381-1169/00/$ - see front matter
PII: S1381-1169(00)00214-4

withdrawing substituents in the porphyrin ring with catalyst immobilisation on inorganic matrices [1–3,7–12]. A new approach consisting of MeP encapsulation in a size- and shape-selective mineral matrix framework such as zeolites, the so-called ship-in-a-bottle system, has been recently developed [13a,b,c,14]. The approach adopted consists of cationic MeP, stabilised by the negative framework from inside the zeolite cavities. Such zeolite-encapsulated MePs present many advantages: (i) zeolites have well-organised nanopores and nanochannels, which readily serve as supporting hosts for various molecules; (ii) the zeolite replaces the protein portion of natural enzymes and provides a controlled steric environment for the MeP, serving as a model for the active site of cytochrome *P*-450 [13a,b,c,14]; (iii) these heterogeneous catalysts can be used in organic media for the oxidation of hydrophobic substrates. Nakamura et al. [15] were the first to describe how iron(III) and manganese(III) 5,10,15,20-tetramethylporphyrin complexes were synthesised within the cages of NaY zeolite and the catalytic activity of these materials in the oxidation of saturated hydrocarbons with hydrogen peroxide was studied. In another report, Battioni et al. [16] have described the catalytic activity of some MePs encapsulated in NH_4Y zeolite, where the porphyrin complexes were synthesised inside the Y zeolite, a method known as the template synthesis method. Balkus et al. [17] have used the zeolite synthesis method to synthesize zeolite NaX around cobalt (II) and copper (II) phthalocyanine complexes. Our group has been working on the synthesis of the NaX zeolite around cationic FePs and has used such catalysts in hydrocarbon oxidation [18]. More recently, the synthesis of a faujasite-Y confined MeP, and its catalytic activity in the oxidation of cyclohexene has been reported [19].

In this work, we describe the use of two different cationic FePs encapsulated in NaX zeolite as catalysts for hydrocarbon oxidation. The heterogeneous FePs were obtained through the zeolite synthesis method, where NaX zeolite was synthesised (I, Fig. 1) around one of the pure cationic FePs: iron(III) 5,10,15,20-tetrakis(4-*N*-methylpyridyl)porphyrin (FeP**1**) (Fig. 1) or iron(III) 5-mono(2,6-dichloro-phenyl)10,15,20-tris(4-*N*-methylpyridyl)porphyrin (FeP**2**) (Fig. 1). The syntheses yielded pure iron(III) porphyrins (FePNaX) catalysts without any by-products blocking the zeolite nanopores. In order to verify the functional model of cytochrome *P*-450 and to know their profile as selective catalyst, these encapsulated FePs were then used in the oxidation of (*Z*)-cyclooctene,

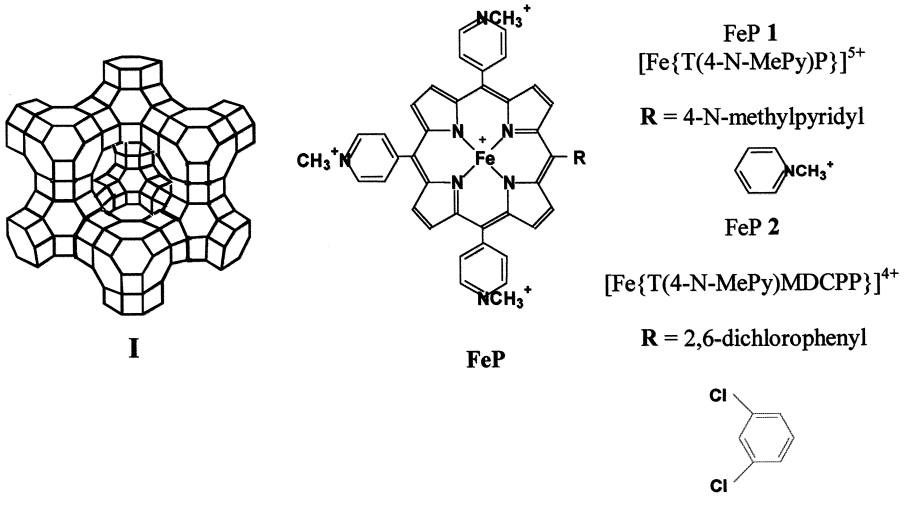

Fig. 1. Zeolite NaX (I) and ironporphyrins (FeP).

cyclohexane and adamantane by iodosylbenzene (PhIO) [20] in organic media.

2. Experimental

2.1. Materials

All solvents and reagents were of commercial grade unless otherwise stated and treated as described before [8a,b]. (*Z*)-Cyclooctene purity was determined by gas chromatographic analysis, and it was purified by column chromatography on basic alumina prior to use.

2.1.1. FePNaX

Fe[T(4-N-MePy)P]Cl$_5$ (FeP**1**, Fig. 1): This FeP was purchased from Midcentury and was used without prior purification.

Fe[T(4-N-MePy)MDCPP]Cl$_4$ (FeP**2**, Fig. 1): The free-base porphyrin T(4-*N*-MePy)MDCPPH$_2$ and the corresponding iron porphyrin were prepared according to the procedure previously described [11a]. Iron insertion into T(4-*N*-MePy)MDCPPH$_2$]Cl$_3$ was achieved by heating the methylated free-base porphyrin and $Fe(NH_4)_2(SO_4)_2 \cdot 6H_2O$ at reflux in water for 2 h. The solution was cooled and $NaClO_4$ was added, producing a dark precipitate. The mixture was chilled for 2 h and the solid FeP was isolated by filtration. The perchlorate anion was exchanged for chloride using an ion exchange resin [11b].

T(4-*N*-MePy)MDCPPH$_2$ and FeP**2** were characterized by TLC, UV-Vis and ^{1}H NMR spectroscopy, FAB mass and ES MS.

T(4-N-Py)MDCPPH$_2$: UV-Vis (DCM) λ_{max}, nm (ε, mol^{-1} l cm^{-1}) 418 (2.5×10^5, Soret band), 512 (1.1×10^4), 588 (7.3×10^3). ^{1}H NMR ($CDCl_3$) $\delta = 9.01$–9.07 (m, 6H 3,5-pyridyl), $\delta = 8.84$ (d, $J = 4.90$ Hz, 2H β-pyrrole), $\delta = 8.83$ (s, 4H β-pyrrole), $\delta = 8.74$ (d, $J = 4.90$ Hz, 2H β-pyrrole), $\delta = 8.16$ (d, $J = 4.40$ Hz, 4H 2,6-pyridyl), $\delta = 8.14$ (d, $J = 4.40$ Hz, 2H 2,6-pyridyl), $\delta = 7.82$ (q AB_2, $J = 8.24$ Hz, 2H 3,5-dichlorophenyl), $\delta = 7.73$ (q AB_2, $J = 8.24$ Hz, 1H 4-dichlorophenyl), $\delta = -2.87$ (s, 2H *N*-H pyrrole), FAB MS [M] = 686, R_f silica/4% MeOH in DCM = 0.56.

T(4-N-MePy)MDCPPH$_2$*Cl*$_3$: UV-Vis (H_2O) λ_{max}, nm (ε, mol^{-1} l cm^{-1}) 422 (1.4×10^5, Soret band), 512 (7.5×10^3), 540 (3.8×10^3), 590 (3.7×10^3). ^{1}H NMR ($CDCl_3$) $\delta = 9.01$–9.07 (m, 6H, 3,5-pyridyl), $\delta = 9.01$–9.16 (m, 8H β-pyrrole), $\delta = 8.92$–$9{,}00$ (m, 6H, 2,6-pyridyl), $\delta = 7{,}99$–8.10 (m, 3H, 3,5-dichlorophenyl and 4-dichlorophenyl), $\delta = 4.74$ (s, 6H, N$^+$-methyl), $\delta = 4.76$ (s, 3H, N$^+$-methyl), $\delta = -3.00$ (s, 2H, pyrrole). ES MS 244.6[(M-3Cl$^-$)/3]; 365.2[(M − 3Cl$^-$)/2]; 358.0[(M − 3Cl$^-$ CH$_3^+$)/2]; 366.2[(M − 3Cl$^-$H$^+$)/2]; 728.4[(M − 3Cl$^-$2H$^+$)]; 383.1[(M − 2Cl$^-$)/2]. R_f silica/4% MeOH in DCM = 0.05.

FeP2: UV-Vis (MeOH) λ_{max}, nm (ε, mol^{-1} l cm^{-1}) 424 (6.6×10^4, Soret band), 560 (5.9×10^3), 594 (5.8×10^3). ES MS 262.3[(M − 4Cl$^-$)/3]; 393.0[(M^{2-} − 4Cl$^-$)/2]; 784.7[(M^{3-} − 4Cl$^-$)]; 273.5[(M − 3Cl$^-$)/3]; 428.5[(M-2Cl$^-$)/2]. R_f silica/4% MeOH in DCM = 0.05.

2.1.2. Preparation of zeolite-encapsulated FeP-NaX

The FePNaX catalysts were synthesised through the method of Balkus et al. [17]. A silicate gel was prepared by stirring 0.70 g silica, 0.60 g NaOH, 3.6×10^{-5} mol of the desired FeP and 1.5 ml H_2O. The gel was then added to an aluminate solution consisting of 1.55 g of aluminum isopropoxide (Al[$(CH_3)_2$-CHO]$_3$), 0.65 g NaOH and 2.0 ml H_2O, and this mixture was transferred to a polypropylene bottle with 6.0 ml H_2O and stirred at room temperature for 24 h. The bottle was put in a water bath at 90°C for 15 h and then 20 ml H_2O was added. The resulting solids were filtered, washed several times with water and dried at 80°C for 24 h. The samples were Soxhlet-extracted with water for 3 days, and then with methanol for another 3 days to remove all the FeP present on the external surface of the zeolite. The samples were dried at 80°C for 24 h.

To calculate the amount of loaded FeP in the zeolite, a known amount of FePNaX was weighed and destroyed with concentrated and heated HCl in order to remove the FeP from the zeolite. UV-Vis spectra of the removed FeP were recorded in aqueous solutions (pH ~ 2) and the absorbance of the Soret band was used to evaluate the loading of FeP per gram of FePNaX, which was 1.10×10^{-6} mol g^{-1} for FeP**1**NaX and 3.85×10^{-6} mol g^{-1} for FeP**2**NaX.

2.2. UV-Vis and EPR

The spectra were recorded as previously described [8a,b].

2.3. ^{1}H NMR spectra

^{1}H NMR spectra were accomplished on a Brüker DR XC 400, 9.4 T spectrometer using TMS as internal reference.

2.4. ES MS spectra

Electrospray mass spectra were recorded on an LCQ Finnigan MAT spectrometer.

2.5. X-ray diffraction powder analysis

X-ray powder diffraction patterns were obtained on an Universal XZG-4C diffractometer using CuK α radiation.

2.6. TGA / DTA analysis

An SDT2960 simultaneous DTA/TGA apparatus from TA Instruments was used to obtain thermogravimetric analyses, where an oxygen flux of 100 ml min^{-1} was used and the heating rate was 10°C min^{-1} until 1000°C.

2.7. N_2 BET surface area determination

Specific surface analyses were performed on a Micromerits ASAP 2000 with nitrogen as the absorption gas.

2.8. Oxidation reactions

Controls for all reactions were carried out in the absence of FeP. The reactions were carried out in a 2-ml vial sealed with Teflon-coated silicone septum. A total of 2.54×10^{-3} mol DCE, the substrate (2.66×10^{-3} mol of cyclohexane or 2.25×10^{-3} mol of (*Z*)-cyclooctene or 8.90×10^{-4} mol of adamantane) and 20 μl internal standard (6.5×10^{-2} mol l^{-1} in DCE) were added to the vial containing 0.0500 g FePNaX and 1.0×10^{-6} mol PhIO under argon. The mixture was protected from light and stirred) at room temperature, for the desired time. The build-up of products was monitored by gas chromatography.

2.9. Product analysis

The products were analyzed by gas chromatography using the internal standard method. Cyclohexanone, *n*-octanol and benzophenone were used as standard in the case of (*Z*)-cyclooctene, cyclohexane and adamantane oxidation, respectively. The yields were based on PhIO. Gas chromatographic analysis were performed on a Varian Star 3400 CX gas chromatograph coupled to a Varian star chromatography workstation. Nitrogen was used as the carrier gas with a hydrogen flame ionization detector. The inox column (length, 30 m; internal diameter, 0.538 mm) was packed with 1-mm-wide DB-WAX film. The attained products were analyzed by comparison of their retention times with authentic samples.

3. Results and discussion

3.1. Synthesis and characterization of the zeolite-encapsulated FePs

The FePNaX catalysts were obtained according to Balkus et al. [17]. The advantage of this zeolite synthesis method over the template synthesis is that an electrostatic interaction is intro-

duced between the host (anionic aluminosilicate species in the zeolite) and the guest (cationic 4-*N*-methylpyridyl substituents on the FePs), enabling the construction of zeolite nanocages around the pure cationic FePs. Unlike the template synthesis method, this approach avoids the presence of free metal ion, free ligand or impurities like polypyrrins (which result from MeP synthesis) [21] in the zeolite cages, which could complicate both characterization (presence of a broad band at $\sim$480nm) and reactivity (pore blockage) of the resulting material.

The FePNaX catalysts obtained were characterized by various techniques such as X-ray powder diffraction, TGA/DTA analysis, N_2 BET surface area, UV-Vis and EPR spectroscopies. Both FePNaX catalysts presented good X-ray powder diffraction patterns, where narrow peaks are in agreement with $2\theta = 27.5°$, 31.5° and 36.6° for the (5 3 3), (6 4 2) and (7 5 1) planes of the NaX zeolite [22], respectively.

TGA/DTA analysis of NaX shows that there is a total mass decrease of 18%, which can be attributed to dehydration. Both FeP**1**NaX and FeP**2**NaX presented a total mass decrease of 22%, due to losses of both water molecules and organic material. N_2 BET surface area experiments show that NaX presents higher surface area (370 $m^2\ g^{-1}$) than the FePNaX catalysts; 345 $m^2\ g^{-1}$ for FeP**1**NaX and 357 $m^2\ g^{-1}$ for FeP**2**NaX. The decrease of surface areas of FeP**1**NaX and FeP**2**NaX could be due to the presence of compounds in the cages of the zeolite [23]. Therefore, both TGA/DTA and N_2 BET surface area techniques support encapsulation of the cationic FePs.

The UV-Vis spectra of both FeP**1**Cl and FeP**2**Cl in aqueous solution is characterized by a broad envelope representing the overlap of two spectral bands in the Soret region. This pattern had already been described before for FeP**1**Cl by Pasternack et al. [24]. FeP**1**Cl has a maximum at 398 nm and a shoulder at 415 nm; FeP**2**Cl has a maximum at 402 nm and a shoulder at 422 nm. Since the spectral patterns for both FePCl complexes are very similar, only the UV-Vis spectrum of FeP**2**Cl is presented in Fig. 2. The FePCl complexes also present absorption bands at 338 and 514 nm (Fig. 2). Concerning the zeolite-encapsulated FePs, they also present a broad envelope Soret band having maxima at 422 and 440 nm (Fig. 2, insert), which are red-shifted if compared to the initial FePCl complexes. Such shift happens possibly because there is a distortion of the porphyrin ring upon FeP encapsulation [17]. The bands at 338 and 514 nm present in the spectra of the FePCl complexes are replaced by a band at 570 nm in the FePNaX complexes (Fig. 2, insert). Based on the studies of Kobayashi et al. [25] and Cheng et al. [26], who attribute the band at $\lambda = 580$ nm present in the spectra of $Fe(TPP)OCH_3$ and Fe(TMP)OH to axial coordination of the FeP to oxygen, we assign the band at $\lambda = 570$ nm in the present study to the axial coordination of the FeP to H_2O or OH-containing ligands present in the zeolite framework. The EPR spectra of both FePNaX catalysts display high-spin Fe^{III} signals in $g_\perp = 6$ and $g_\parallel = 2$. In fact, our group has recently published an article showing that high-spin FePOH complex also display EPR signals in $g_\perp = 6$ and $g_\parallel = 2$ and UV-Vis band at $\lambda = 576$ nm [27].

When the FePs were removed from the zeolite by destroying the mineral lattice with HCl, the absorption spectra obtained were analogous

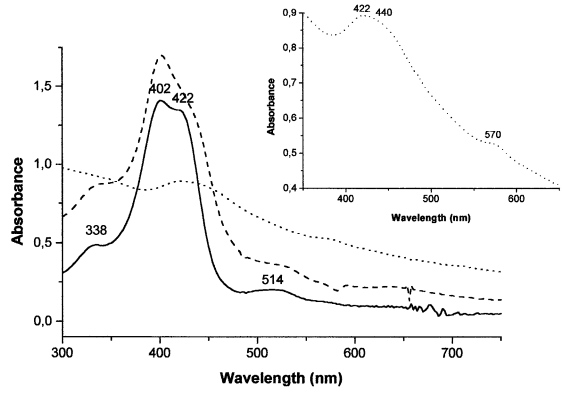

Fig. 2. UV-Vis spectra of FeP**2**NaX (dotted line), FeP**2** in H_2O before encapsulation (full line) and FeP**2**NaX after zeolite digestion with HCl (traced line). Insert: FeP**2**NaX.

to those of the corresponding FePCl complexes. The UV-Vis spectrum of FeP**2**Cl in aqueous solution at pH ~ 2 resulting from the FeP**2**NaX zeolite digestion is shown in Fig. 2 as an example. Such results indicate that the reaction media of the zeolite synthesis did not destroy the FePs.

3.2. FePNaX-catalyzed hydrocarbon oxidation by PhIO in organic media

3.2.1. FePNaX-catalyzed (Z)-cyclooctene epoxidation

For the initial studies on the catalytic activity of FeP**1**NaX and FeP**2**NaX, the epoxidation of (*Z*)-cyclooctene by PhIO was selected to compare the efficiency of these encapsulated catalysts with each other and with analogous homogeneous systems. This substrate was chosen for three reasons: (i) it gives a clean conversion into *cis*-epoxycyclooctane without contamination from other alkene oxidation products; (ii) it is easily oxidized, thus preventing loss of the active catalytic intermediate through competitive reactions with PhIO and the FeP itself; (iii) it has been extensively used in earlier MeP-catalysed oxidation reactions [28,29]. PhIO was chosen as oxygen source since (i) it can give good oxidant conversions, (ii) it is relatively inert in the absence of FeP, (iii) it reacts with FeP generating the $Fe^{IV}(O)P^{\cdot+}$ active catalytic species and PhI [28,30]. In homogeneous system, FeP**1** is reported to lead to 50% *cis*-epoxycyclooctane yield in the epoxidation of (*Z*)-cyclooctene by PhIO, in MeOH [31] (Table 1; Fig. 3). As for FeP**2**, our group [11a,b] has found that it leads to 60% epoxide yield when the reaction is performed in 30% ACN in DCE (Table 1). However, the use of MeOH or ACN as reaction media presents a major drawback: both solvents can be oxidized by the active species $Fe^{IV}(O)P^{+}$, competing with the substrate [32,33]. Replacing these solvents by DCE, which is less liable to oxidation by the FeP, is not possible because the cationic FeP**1** and FeP**2** are not soluble in it. Use of these catalysts in aqueous solution is also not advantageous since (*Z*)-cyclooctene is not soluble in this medium. The synthesis of zeolite NaX around the cationic water soluble FeP**1** and FeP**2** is therefore very important because it produces the heterogeneous encapsulated catalysts, FeP**1**NaX and FeP**2**NaX, which enable the use of these FePs as catalysts for the oxidation of hydrophobic organic substrates in organic medium.

Table 1
Catalytic Activity of FeP**1**NaX and FeP**2**NaX in the oxidation of cyclohexane, adamantane and (*Z*)-cyclooctene by PhIO

Catalyst	Substrate	Product yields (%)[a]		
	(*Z*)-cyclooctene	Cox		
FeP**1**		50[b]		
FeP**1**NaX		86		
FeP**2**		60[c]		
FeP**2**NaX		95		
	Cyclohexane	C_6-ol	C_6-one	C_6-ol/C_6-one
FeP**1**		11	10	
FeP**1**NaX		50	5	2.8[d]
FeP**2**NaX		25	21	1.2
	adamantane	Ad-1-ol	Ad-2-ol	Ad-1-ol/Ad-2-ol[e]
FeP**1**NaX		45	7	20
FeP**2**NaX		35	10	11

Conditions: Argon atmosphere; $T = 25$°C; magnetic stirring; substrate/solvent /PhIO/FeP molar ratio = 1.5×10^{4}:5.1×10^{3}:20:1; [FeP] ~ 1×10^{-4} mol l^{-1} in 1,2-dichloroethane.

[a] Based on PhIO.
[b] FeP in MeOH [18].
[c] FeP in 30% ACN in DCE.
[d] FeP in ACN [6].
[e] Statistically corrected.

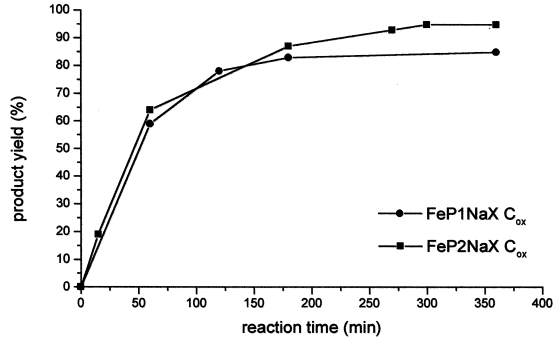

Fig. 3. Build-up of Cox in the FePNaX-catalyzed oxidation of (*Z*)-cyclooctene.

FeP**1**NaX and FeP**2**NaX efficiently catalysed the epoxidation of (*Z*)-cyclooctene by PhIO in DCE, giving rise to *cis*-epoxycyclooctane yields of 85% and 95%, respectively (Table 1). These results are far better than those obtained in homogeneous systems (Table 1), which were carried out in MeOH for FeP**1** (50%) and in ACN/DCE for FeP**2** (60%). Besides the absence of competitive solvent oxidation with pure DCE, the encapsulation of FePs renders them more resistant to oxidative self-destruction. FeP**2**NaX gives higher epoxide yields than FeP**1**NaX since the presence of the electron-withdrawing chloro substituents in the former catalyst make it more electrophilic and thus more reactive towards the electron-rich olefin.

3.2.2. FePNaX-catalyzed cyclohexane oxidation

In the cyclohexane oxidation using cationic FeP**1** and FeP**2** as catalysts in polar solvents such as MeOH and ACN, the solvent competitive oxidations are favoured [8a], since the cyclohexane is much more inert than cyclooctene. In the oxidation of cyclohexane by PhIO in homogeneous system (ACN), FeP**1** is reported to lead to a cyclohexanol (C_6-ol) yield of 11% and a C_6-ol/C_6-one ratio of 2.8 [6] (Table 1; Fig. 4). The homogeneous system reactions cannot be reproduced in DCE where FeP**1** and FeP**2** are insoluble. In this way, only the encapsulated systems as catalysts will be presented in this study, using DCE as solvent. When the reaction is catalysed by the heterogeneous catalyst FeP**1**NaX in DCE, a C_6-ol yield of 50% and a C_6-ol/C_6-one ratio of 10 is obtained (Table 1), showing that the encapsulated FeP**1** is a more efficient and selective catalyst than its homogeneous analog. In this case, the hydroxylation occurs according to step 2 (Scheme 1). Here, the $Fe^{IV}(O)P^{\cdot+}$ species abstract hydrogen from the substrate, forming a solvent cage, followed by the rapid transfer of the hydroxyl group from Fe^{IV}(OH)P to the cyclohexyl radical ($R^{\cdot}$), the so-called oxygen rebound mechanism (path **a**, Scheme 1) [34]. This is expected for a *P*-450 model system.

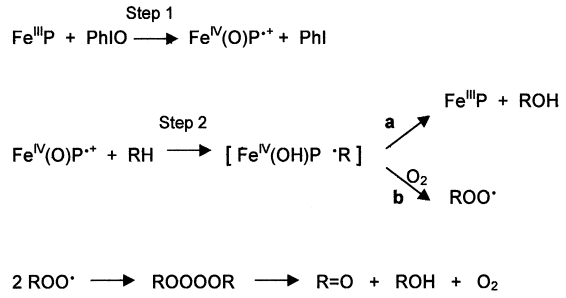

Scheme 1.

FeP**2**NaX, on the other hand, is less selective for cyclohexane oxidation than FeP**1**NaX (C_6-ol yield = 25% and C_6-ol/C_6-one = 1.2, Table 1). One possible explanation for these results is that the 2,6-dichlorophenyl substituent renders FeP**2** more bulky and, therefore, it may lead to an obstruction of the pores in the zeolite-encapsulated FeP. This might hinder the access of the substrate to the active site of the catalyst and when cyclohexane reaches the FeP, it is oxidized to the corresponding alcohol by the $Fe^{IV}(O)P^{\cdot+}$ species (path **a**, Scheme 1) and then over-oxidized to ketone, before diffusing back to the solution. A more likely explanation is that a Russell-type mechanism involving O_2 imprisoned within the zeolite cages (path **b**, Scheme 1) may be operating parallel to path **a**. The cyclohexyl radicals ($R^{\cdot}$) may escape from the solvent cage and react with the oxygen, to give

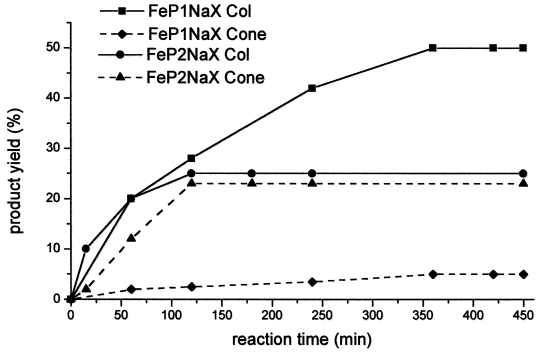

Fig. 4. Build-up of C_6-ol and C_6-one in the FePNaX-catalyzed oxidation of cyclohexane.

a secondary peroxyl radical ($ROO^{\cdot}$). The termination of two $ROO^{\cdot}$ radicals would then give the tetraoxide ROOOOR, which would generate both C_6-ol and cyclohexanone, as well as additional O_2 in the reaction site [35a,b]. A fact that reinforces this second explanation is that a roughly 1:1 stoichiometric amount of C_6-ol and cyclohexanone is obtained at the end of the oxidation reaction. In fact, Battioni et al [16] have already reported that zeolite-encapsulated iron(III) 5,10,15,20-tetramethylporphyrin also leads to a C_6-ol/C_6-one ratio of 1:1 when the oxidation reaction is carried out with oxygen under normal pressure.

3.2.3. Adamantane oxidation

In the oxidation of adamantane by PhIO, both FePNaX catalysts give 1-adamantanol (Ad-1-ol) and 2-adamantanol (Ad-2-ol) as products. 2-Adamantanone (Ad-2-one) is not obtained in any of the cases. The total alcohol yields are 52% and 45% for Fe**P1**NaX and Fe**P2**NaX, respectively (Table 1; Fig. 5). Therefore, despite having electron-withdrawing substituents in its porphyrin ring, Fe**P2**NaX is not as efficient as Fe**P1**NaX for adamantane oxidation. This happens probably because the chloro substituents in the former catalyst hinder the approach of the bulky adamantane to the active site of the FeP.

Concerning selectivity, Fe**P1**NaX and Fe**P2**NaX give an Ad-1-ol/Ad-2-ol ratio of 20:1 and 11:1, respectively (after statistical correction), showing a preferable alkane oxidation at the tertiary C–H bond (C^{terc}). So these results indicate a free radical activation of the C–H bonds of adamantane, as is expected for a *P*-450 model [36].

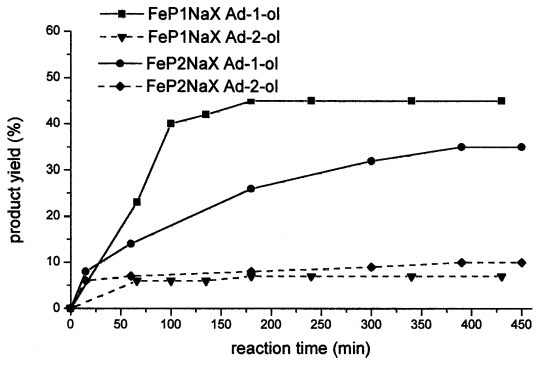

Fig. 5. Build-up of Ad-1-ol and Ad-2-ol in the FePNaX-catalysed oxidation of adamantane.

4. Conclusion

The approach adopted herein for the obtention of zeolite-encapsulated FePs led to clean syntheses of the desired catalysts. The preliminary results reported in this work are very encouraging since they show that, through suitable choice of substituents on the porphyrin ring and substrates, it is possible to obtain different size- and shape-selectivity in the reactions studied. It is also shown that the efficiency and selectivity of the encapsulated FePs are sensitive to electronic and steric effects of the substituents present in the porphyrin ring.

In homogeneous systems, these cationic FeP do not work as catalyst for alkane oxidation in DCE. When encapsulated, they are particularly efficient in DCE. The Fe**P1**NaX system consists of a polar hemin in isolated sites, which selectively catalyse cyclohexane oxidation in apolar solvent. In the same way, the active site of *P*-450 is a polar protohemin in a hydrophobic pocket that promotes selective cyclohexane oxidation [37]. Therefore, FePNaX catalysts represent good cytochrome *P*-450 model systems, since (i) they efficiently epoxidize cyclooctene and (ii) preferably hydroxylate adamantane at the tertiary C–H bond, indicating that there is an hydrogen abstraction through the $Fe^{IV}(O)P^{\cdot+}$ species in the initial step (Scheme 1).

However, the results have indicated that dioxygen confined in the zeolite cavities may be involved in the cyclohexane oxidation catalysed by Fe**P2**NaX, which has one 2,6-dichlorophenyl group replacing methyl pyridyl. In this case, instead of the oxygen rebound mechanism (path

a, Scheme 1), the cyclohexyl radical escapes from the solvent cage formed after the $Fe^{IV}(O)P^{\cdot+}$ species abstracts hydrogen. The radical may then readily react with dioxygen, initiating the Russell-type mechanism. Further studies using other zeolite-encapsulated MePs are underway in our laboratories so as to understand better the factors that influence the various oxidation systems.

Acknowledgements

We thank CAPES, CNPq and FAPESP for financial support and Prof. B. Meunier for helpful discussions. We also thank Prof. A.G. Ferreira for the NMR spectra, Prof. J.R. Lindsay-Smith for the ES MS spectra and Prof. O.R. Nascimento for the EPR spectra.

References

[1] B. Meunier, Chem. Rev. 92 (1992) 1411.
[2] J.R. Lindsay-Smith, R.A. Sheldon (Eds.), Metaloporphyrin in Catalytic Oxidations, Marcel Dekker, New York, 1994, Chap. 11.
[3] B. Meunier, in: F. Montanari, L. Casella (Eds.), Mettaloporphyrins Catalyzed Oxidations, Kluwer Academic Publishers, Dordrecht, 1994, Chap. 1.
[4] D.R. Leanord, J.R.L. Smith, J. Chem. Soc., Perkin Trans. 2 (1992) 2187.
[5] L. Barloy, J.P. Lallier, P. Battioni, D. Mansuy, Y. Piffard, M. Tournoux, J.B. Valim, W. Jones, New J. Chem. 16 (1992) 71.
[6] Y. Iamamoto, Y.M. Idemori, S. Nakagaki, J. Mol. Catal. A: Chem. 99 (1995) 187.
[7] P. Battioni, E. Cardin, M. Louloudi, B. Schollhorn, G.A. Spyroulias, D. Mansuy, T.G. Traylor, Chem. Commun. (1996) 2037.
[8a] Y. Iamamoto, K.J. Ciuffi, H.C. Sacco, L.S. Iwamoto, O.R. Nascimento, C.M.C. Prado, J. Mol. Catal A: Chem. 109 (1996) 189.
[8b] Y. Iamamoto, H.C. Sacco, K.J. Ciuffi, L.S. Iwamoto, O.R. Nascimento, C.M.C. Prado, J. Mol. Catal. A:Chem. 116 (1997) 405.
[9] M.D. Assis, J.R.L. Smith, J. Chem. Soc., Perkin Trans. 2 (1998) 2221.
[10] K.J. Ciuffi, H.C. Sacco, J.B. Valim, C.M.C.P. Manso, O.A. Serra, O.R. Nascimento, E.A. Vidoto, Y. Iamamoto, J. Non-Cryst. Solids 247 (1999) 146.
[11a] C.M.C. Prado-Manso, E.A. Vidoto, F.S. Vinhado, H.C. Sacco, K.J. Ciuffi, P.R. Martins, A.G. Ferreira, J.R. Lindsay-Smith, O.R. Nascimento, Y. Iamamoto, J. Mol.Catal. A Chem. (1999) in press.
[11b] P. Bigey, S. Frau, C. Loup, C. Claparols, J. Bernadou, B. Meunier, Bull. Soc.: Chim. 133 (1996) 679.
[12] J.P. Collman, X. Zhang, V.J. Lee, E.S. Uffelman, J.I. Brauman, Science 261 (1993) 1404.
[13a] D. Mansuy, Coord. Chem. Rev. 125 (1993) 129.
[13b] K.D. Karlin, Science 261 (1993) 701.
[13c] F. Bedioui, Coord. Chem. Rev. 144 (1995) 39.
[14] I. Stiefel, in: J. Reedijk, E. Bouwman (Eds.), Bioinorganic Catalysis, Marcel Dekker, New York, 1999, Chap. 3.
[15] M. Nakamura, T. Tatsumi, H. Tominaga, Bull. Chem. Soc. Jpn. 63 (1990) 3334.
[16] P. Battioni, R. Iwanejko, D. Mansuy, T. Mlodnicka, J. Poltowicz, F. Sanchez, J. Mol. Catal. A: Chem. 109 (1996) 91.
[17] K.J. Balkus Jr., A.G. Gabrielov, S.L. Bell, F. Bedioui, L. Roué, J. Devynck, Inorg. Chem. 34 (1994) 67.
[18] I.L.V. Rosa, O.A. Serra, C.M.C.P. Manso, Y. Iamamoto, Book of Abstracts of the 9th International Symposium on Relations Between Homogeneous and Heterogeneous Catalysis, University of Southampton, UK, 1998, p. 131.
[19] B.Z. Zhan, X.Y. Li, Chem. Commun. (1998) 349.
[20] J.G. Sharefkin, H. Saltzmann, Org. Synth. 43 (1963) 62.
[21] J.S. Lindsey, R.W. Wagner, J. Org. Chem. 54 (1989) 828.
[22] C.V. McDaniel, P.K. Maher, in: J.A. Rabo (Ed.), Zeolite Chemistry and Catalysis, ACS, Washington, DC, 1976, Chap. 4.
[23] E. Paez-Mozo, N. Gabrinnas, F. Lucaccioni, D.D. Acosta, P. Patrono, A. La Ginestra, P. Ruiz, B. Delmon, J. Phys. Chem. 97 (1993) 12819.
[24] R.F. Pasternack, H. Lee, P. Malek, C. Spencer, J. Inorg. Nucl. Chem. 39 (1977) 1865.
[25] H. Kobayashi, Y. Yanagawa, Osada, S. Minami, M. Shimizu, Bull. Chem. Soc. Jpn. 46 (1973) 1471.
[26] R. Cheng, L. Latos-Grazynski, A.L. Balch, Inorg. Chem. 21 (1982) 2412.
[27] C.M.C.P. Manso, C.R. Neri, E.A. Vidoto, H.C. Sacco, K.J. Ciuffi, L.S. Iwamoto, Iamamoto, O.R. Nascimento, O.A. Serra, J. Inorg. Biochem. 73 (1999) 85.
[28] P.R. Cooke, J.R.L. Smith, J. Chem. Soc., Perkin Trans. 1 (1994) 1913.
[29] K.A. Lee, W. Nam, J. Am. Chem. Soc. 119 (1997) 1916.
[30] C. Gilmartin, J.R.L. Smith, J. Chem. Soc., Perkin Trans. 2 (1995) 243.
[31] D.R. Leanord, J.R.L. Smith, J. Chem. Soc., Perkin Trans. 2 (1990) 1917.
[32] D.R. Leanord, J.R. Lindsay-Smith, J. Chem. Soc. Perkin Trans. 2 (1991) 25.
[33] B. Meunier, in: R.A. Sheldon (Ed.), Metalloporphyrins in Catalytic Oxidations, Marcel Dekker, New York, 1994, Chap. 5.

[34] J.T. Groves, Cytochrome *P*450 structure, in: P.R.O. Montellano (Ed.), Mechanism and Biochemistry, Plenum Press, New York, 1995, p. 3, Chap. 1.
[35a] P.A.M. MacFaul, I.W.C.E. Arends, K.U. Ingold, D.D.M. Wayner, J. Chem. Soc., Perkin Trans. (1997) 135.
[35b] J. Kim, C. Kim, R.G. Harrison, E.C. Wilkinson, L. Que Jr., J. Mol. Catal. A: Chem. 117 (1997) 83.
[36] P. Hoffmann, A. Robert, B. Meunier, Bull. Soc. Chim. Fr. 129 (1992) 85.
[37] J.H. Dawson, Science 240 (1988) 433.